Computation of Inter-turn Voltages in Transformer Windings with Interconnected Distribution Cable

G. Hoogendorp, M. Popov, L. van der Sluis

Abstract—**The paper deals with the use of the hybrid model to compute inter-turn voltages in transformer windings when a distribution cable is connected to the transformer. This model uses a combination of a single-transmission line model (STLM) and a multiconductor transmission line model (MTLM). It is shown that the hybrid model can be used with full success for computation of inter-turn voltage distribution in layer-type distribution transformers. Measured voltages at specific taps are compared with the computed voltages when a pulse with a short rise time is applied at the transformer terminal. In this work, the influence of the cable on the voltage distribution in transformer windings will be analyzed.**

Keywords: **Fast transients, modified Fourier transformation, transfer function, dielectric relaxation, complex permittivity.**

I. INTRODUCTION

COMPUTATION of inter-turn voltages in transformers is of great importance for the design of transformer insulation. During fast surges like lightning and switching the transformers, very fast transients take place which result in an increase of the inter-turn voltages. Switching operations in a gas insulated substation (GIS) are also known to produce very fast transient overvoltages (VFTO's) which are dangerous for the transformer insulation. Also, in medium voltage systems where vacuum circuit breakers are used [1,2], high-frequency oscillations occur which can be dangerous because of their short rise time. Another problem is the external resonance which occurs when the natural frequency of the cable matches the natural frequency of the transformer [3]. Most of the time, the greatest problem is the internal resonance which might occur when the frequency of the input surge is equal to some of the resonance frequencies of the transformer. The experience shows that VFTO's within GIS can be expected to have even a rise time of 0,1 μs and an amplitude of 2.5 p.u. [4]. The inter-turn insulation is particularly vulnerable to high-frequency oscillation, and therefore, the study of the distribution of inter-turn overvoltages is of essential interest. In this work, an accurate computation of voltage transients is done by making use of the hybrid model based on simplified Telegrapher's equations. It is verified that this way of modeling can also be used for layer type transformers with full success. First we consider the situation when an approximated

G. Hoogendorp, M. Popov and L. van der Sluis are with the Delft University of Technology, Power Systems Laboratory, Mekelweg 4, 2628 CD Delft, The Netherlands e-mail: G.Hoogendorp@tudelft.nl; M.Popov@tudelft.nl; L.vanderSluis@tudelft.nl).

step voltage is applied directly to the transformer winding and compute the inter-turn voltages. Then, inter-turn voltage computations are accomplished for a medium voltage distribution cable connected to the transformer.

II. METHODOLOGY

When every turn in a transformer is represented by a transmission line, the computation of the waveforms in each turn is done by the modified Telegrapher's equations described through equation:

$$\frac{\partial \mathbf{V_t}}{\partial x} = -\mathbf{L}\left(\frac{\partial \mathbf{I_t}}{\partial t}\right)$$

$$\frac{\partial \mathbf{I_t}}{\partial x} = -\mathbf{C}\left(\frac{\partial \mathbf{V_t}}{\partial t}\right) + Co[1]\frac{\partial Eo}{\partial t} \qquad (1)$$

$\mathbf{V_t}$ and $\mathbf{I_t}$ are the voltage and current vectors respectively, while $\mathbf{L}$ is the inductance matrix and $\mathbf{C}$ the capacitance matrix. Both are square matrices and their order is equal to the number of turns in a layer. C_0 and E_0 denote the capacitance from a turn to the transformer static plate and excitation voltage respectively. The solutions for the voltage and current in a winding section i of the modified Telegrapher's equations for the STLM model are [5]:

$$V_i(x) = k_i E_o + A_i \exp(-\Gamma(\omega)x) + B_i \exp(\Gamma(\omega)x)$$

$$I_i(x) = \frac{1}{z_i}\left(A_i \exp(-\Gamma(\omega)x) - B_i \exp(\Gamma(\omega)x)\right) \qquad (2)$$

For the MTLM, the solutions for the voltages and currents in each turn in a winding section can be expressed by [5]:

$$V_t(x) = k_i E_o + A_t \exp(-\Gamma(\omega)x) + B_t \exp(\Gamma(\omega)x)$$

$$I_t(x) = v_s[\mathbf{C}]\left(A_t \exp(-\Gamma(\omega)x) - B_t \exp(\Gamma(\omega)x)\right) \qquad (3)$$

Where constants A_t and B_t can be calculated by equalizing the voltages and currents at the end of one line with the beginning of the next line, and k_i is the capacitive distributed voltage, which is due to the existing capacitances between the layers and between layers and ground. The propagation constant Γ in the above voltage equation can be approximated by:

$$\Gamma = \frac{1}{v_s d}\sqrt{\frac{\omega}{2\sigma\mu} + \frac{\omega\tan\delta}{2v_s} + \frac{j\omega}{v_s}} \qquad (4)$$

where:

v_s propagation speed of the surge (m/s)

d distance between the conductors (m)

μ magnetic permeability (H/m)

σ conductivity of the conductor (S/m)

The frequency-dependent losses in the winding are taken into account in the first term of (4). The $\tan\delta$ in the second term represents the dielectric losses and is chosen to be 0.05. This is the maximum value that $\tan\delta$ can have for the chosen insulation. The last term is the phase shift during the propagation. The characteristic impedance z_i of a turn in layer i can be estimated by:

$$z_i = \frac{1}{v_s\left(C_o+C_1+K\left(1-\cos\left(\dfrac{\omega a}{v_s}\right)\right)\right)} \quad (5)$$

where a is the length of a turn in the winding section in meters. C_0 and C_1 form the static capacitances [6], K are capacitances between the turns.

Because of the frequency dependence of the transformer parameters, the equations in (1) are solved in the frequency domain. The observed frequency range is from 0 up to 100 MHz. This frequency range is divided into equal steps of 10 KHz, so there are 10001 frequency points in total. For each frequency step, we calculate the propagation constant and the characteristic impedance using (4) and (5) respectively.

The Hybrid Model is applied in the following way. First, the transformer windings are divided into groups. For simplicity we choose the same number of groups with a same number of turns within a group. Then, the voltages at the end of each group are calculated by applying the STLM model. This means that a layer is considered as one transmission line. The constants A_t and B_t in (2) are determined by using the fact that the voltage at the end of the layer is equal to those at the beginning of the next layer. This result in a set of equations in matrix form [6]:

$$\begin{bmatrix} \mathbf{AU(j\omega)} & \mathbf{BU(j\omega)} \\ \mathbf{AI(j\omega)} & \mathbf{BI(j\omega)} \end{bmatrix}\begin{bmatrix} \mathbf{A(j\omega)} \\ \mathbf{B(j\omega)} \end{bmatrix}=\begin{bmatrix} \mathbf{RU(j\omega)} \\ \mathbf{RI(j\omega)} \end{bmatrix} \quad (6)$$

The vector with constants in (6) can now be solved by taking the inverse of the matrix. With these constants, the voltages transfer functions of the layers can be computed using (2) by taking the source equal to unity. The voltages are then just the multiplication of these transfer functions with the input excitation function. Knowing the voltages at the beginning and at the end of each layer, the MTLM can be applied by taking into account that each turn is now a separate line. This method significantly reduces the number of equations and the problem is solved in two steps. The dimension of the **C** matrix in this case will be equal to the number of turns in a specific group. The computation of the turn voltages is performed in a similar way by application of (3) for each turn [6].

$$\begin{bmatrix} \mathbf{MA(j\omega)} & \mathbf{MB(j\omega)} \\ \mathbf{MC(j\omega)} & \mathbf{MD(j\omega)} \end{bmatrix}\begin{bmatrix} \mathbf{A_t(j\omega)} \\ \mathbf{B_t(j\omega)} \end{bmatrix}=\begin{bmatrix} \mathbf{UA(j\omega)} \\ \mathbf{UB(j\omega)} \end{bmatrix} \quad (7)$$

The elements of (6) and (7) are given in the Appendix. The size of this matrix will be twice the number of turns. The vector with constants in (7) can be determined in a similar way as in the STLM. Then the turn voltages need to be transformed back to the time domain by applying the Modified Inverse Fourier Transform:

$$V(t) = \frac{2\exp(bt)}{\pi}\int_0^\Omega \frac{\sin\left(\dfrac{\pi\omega}{\Omega}\right)}{\dfrac{\pi\omega}{\Omega}}\mathrm{Re}(V(j\omega))\cos(\omega t)d\omega \quad (8)$$

For an accurate time domain response, the smoothing constant b, the interval of integration and the step frequency size must be chosen properly [7]. With the computed results in the time domain, the inter-turn voltages can be obtained easily taking the difference between the turn voltages. The used algorithm is depicted in Fig. 10 in the Appendix [5].

III. VERIFICATION OF THE MODEL

The studied transformer is a 15kVA single-phase layer-type distribution transformer, with a transformer ratio 6600V/69V. This transformer consists of 15 layers with 200 turns in each layer. In Table 1 the available data of the studied transformer is shown.

TABLE I
TRANSFORMER DATA

Inner radius of HV winding	73.3 mm
External radius of HV winding	97.4 mm
Inner radius of the LV winding	51 mm
External radius of LV winding	67.8 mm
Wire diameter	1.16 mm
Double wire insulation	0.09 mm
Distance between layers	0.182 mm
Coil's height	250mm
Top / bottom distance from the core	10 mm
Dielectric Permittivity of oil	2.3
Dielectric Permittivity of wire insulation	4

To verify the model, we compare some measurements with computations. Fig. 1 shows the comparison between the measured and computed voltage wave forms at specific turns. Voltages are measured at the 100th and the 200th turn which correspond to the middle turn and last turn of the first layer, and 400th turn which correspond to the last turn of the second layer. There is a good agreement between the measured and computed results.
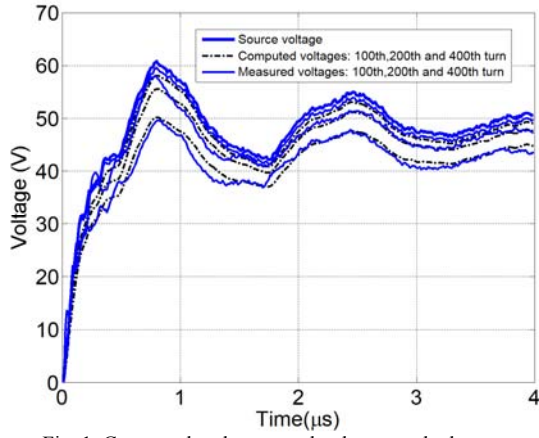
Fig. 1. Computed and measured voltages at the layers.

The time responses are computed for the first 2 μs with an approximated step function with a rise time of 100 ns. Figures 2 and 3 show the inter-turn voltage distribution in the first 20 turns and from 120th to 140th turn in the first layer. Figures 4 and 5 show the computed results of the voltages at specific turns in the second layer.
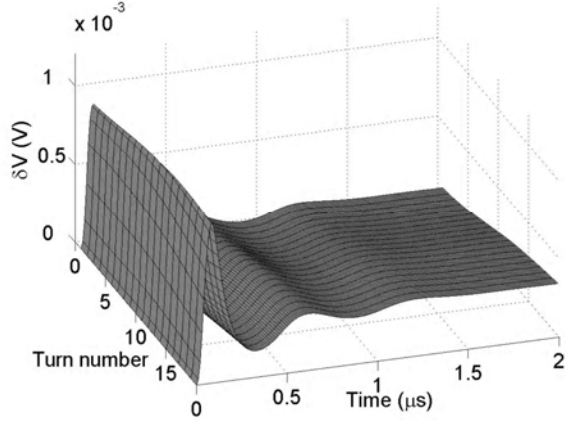

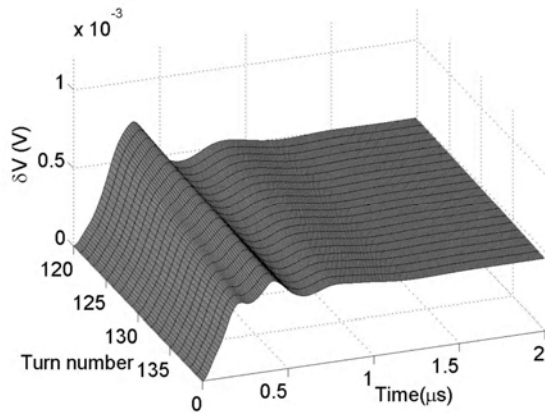Fig. 2. Computed inter-turn voltage distribution of turn 1-20 in the first layer.

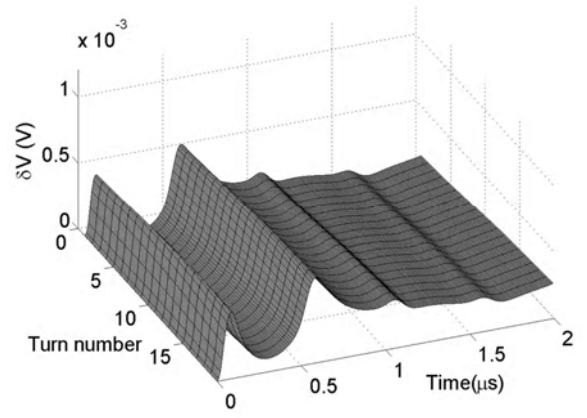Fig. 3. Computed inter-turn voltage distribution of turn 120-140 in the first layer.

Fig. 4. Computed inter-turn voltage distribution of turn 1-20 in the second layer.
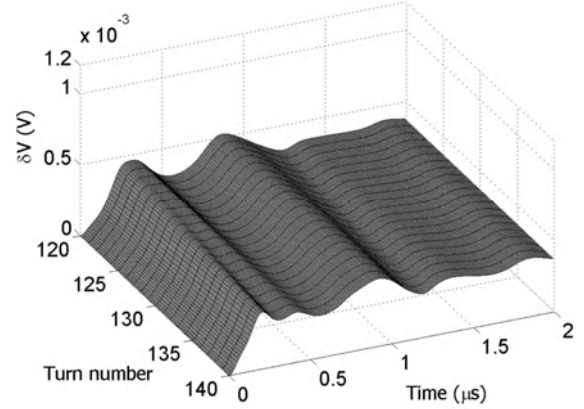

Fig. 5. Computed inter-turn voltage distribution of turn 120-140 in the second layer.

IV. CABLE MODEL

The cable model is represented in a way to determine the propagation constant and eventually the transfer function. In [8], high frequency measurements on this type of XLPE cable are done to extract the material properties. The results of these measurements are fitted by two Cole-Cole functions and a low frequency term with the following dielectric response model:

$$\varepsilon = \frac{A_1}{1 + j\omega\tau_1^{1-\alpha_1}} + \frac{A_2}{1 + j\omega\tau_2^{1-\alpha_2}} + \frac{\sigma_{dc}}{j\omega\varepsilon_0} \qquad (9)$$

This means that the properties of the materials of the cable are modeled by a complex permittivity. Expression (9) is the dielectric relaxation model that describes the permittivity in the frequency domain. The last term accounts for the properties at low frequencies. The values for the parameters for the dielectric relaxation used in (9) are given in Table 2 [8]. The time constants τ_1 and τ_2 are the characteristic relaxation times of the medium. A_1 and A_2 are amplitude factors which are the differences between the low frequency and high frequency permittivities of the material. The factors α_1 and α_2 are mathematical factors denoting the angle of tilt. The low-frequency conductivity of the material is modeled by σ_{dc}. Table 3 does not contain the parameters of the XLPE

insulation material. This material has been modelled by $\varepsilon' = 2.3$ and $\varepsilon'' = 0.001$ [8].

TABLE 2
DIELECTRIC PARAMETERS

Parameter	Inner	Outer	Outer-outer
τ_1 (s)	1×10^{-6}	1×10^{-7}	5×10^{-8}
τ_2 (s)	4×10^{-9}	4×10^{-9}	3×10^{-8}
A_1	500	215	800
A_2	360	170	1000
α_1	0.3	0.3	0.3
α_2	0.3	0.3	0.3
σ_{dc} (mS/m)	6	5.5	800

The dimensions of the used cable are shown in Table 3. The studied cable consists of an aluminium conductor, an inner semi-conducting layer over the conductor, the XLPE insulation, an outer semi-conducting layer, an outer-outer semi-conducting layer and a copper conductor screen.

TABLE 3
CABLE DIMENSIONS

Type	YMeKrvaslqwd 6/10 kV
Length (m)	100
Inner conductor diam. (mm)	17.1
Inner semicon (mm)	1
Insulation XLPE (mm)	3.4
Outer semicon (mm)	0.5
Outer-outer semicon (mm)	0.5
Copper wire shield (mm)	1
Outer sheath (mm)	69

The aluminum conductor and the copper conductor screen form the total series impedance given by [8]:

$$Z_{total} = \frac{1}{2\pi r_1}\sqrt{\frac{j\omega\mu_o}{\sigma_1}} + \frac{j\omega\mu_o}{2\pi}\ln\left(\frac{r_6}{r_1}\right) + \frac{1}{2\pi r_6}\sqrt{\frac{j\omega\mu_o}{\sigma_6}} \quad (10)$$

The first and last terms of (10) accounts for the resistance and the internal inductance of the conductor and the copper screen respectively, which depends on the frequency due to the skin effect. The second term represents the geometric inductance of the cable. The semi-conducting layers and the XLPE insulation can be seen as admittances which are connected in series. The admittance of a semi-conducting layer i is expressed by:

$$Y_i = j\omega\frac{2\pi\varepsilon_0\varepsilon_k}{\ln\left(\dfrac{r_k}{r_{k-1}}\right)} \quad (11)$$

where ε_k is the complex permittivity from (9) and can be written as:

$$\varepsilon(\omega) = \varepsilon'(\omega) - j\varepsilon''(\omega) \quad (12)$$

The total admittance of all n layers together is then shown by:

$$Y_{total} = \frac{1}{\displaystyle\sum_{i=1}^{n}\left(\dfrac{1}{Y_i}\right)} \quad (13)$$

The propagation constant can be derived from the total impedance and admittance following:

$$\Gamma(\omega) = \sqrt{Y_{total}Z_{total}} = \alpha + j\beta \quad (14)$$

In (13) α is the attenuation constant and β is the phase constant. The propagation speed v_s is given by:

$$v_s = \frac{\omega}{\beta} \quad (15)$$

This propagation speed in frequency domain is shown in Fig. 6.
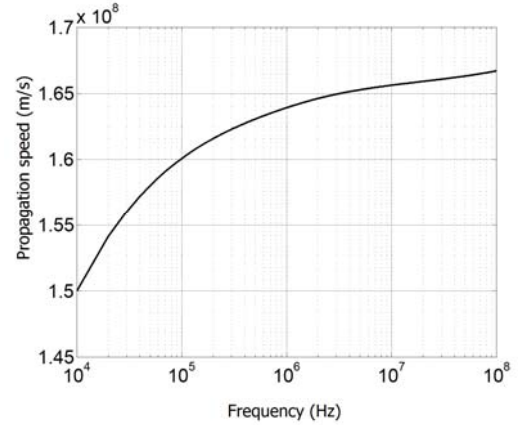

Fig. 6. Calculated propagation speed in the cable.

The frequency dependence of the cable transmission parameters results in a transfer function in the frequency domain. We consider the cable as a transmission line so the Telegrapher's equations can be applied. To solve these equations we define two boundary conditions. At the sending end of the cable (terminal) the voltage is equal to the source voltage, say $g(t)$. When the length of the cable is infinite, the voltage wave is completely damped out. We can write for these conditions:

$$V(0,t) = g(t) \quad (16)$$

$$V(\infty,t) = 0 \quad (17)$$

At time instant zero, the voltage at the beginning of the cable is zero so for the initial condition we write:

$$V(x,0) = 0 \quad (18)$$

Using these conditions the particular solution of the Telegrapher's equations for the voltage wave in the cable in the frequency domain is:

$$V(x, j\omega) = G(j\omega)e^{-\Gamma(\omega)x} \qquad (19)$$

In (18) $\Gamma(\omega)$ is the propagation constant calculated by (13) and $G(j\omega)$ denotes the source voltage in frequency domain. From (18), it follows that the transfer function in frequency domain of the cable is equal to:

$$H_{cable}(j\omega) = \frac{V(x, j\omega)}{G(j\omega)} = e^{-\Gamma(\omega)x} \qquad (20)$$

V. COMPUTATION METHODOLOGY WITH CABLE ADDED

The inner conductor of the cable described is considered to be connected to the transformer primary winding. With the cable transfer function derived in previous section the computation model can be described. In Fig. 7 the block diagram of the model used to obtain the inter-turn voltages in the situation with the inter-connected cable is depicted.

$E_0(j\omega)$ —— [$H_{cable}(j\omega)$] —— [$H_{trafo}(j\omega)$] —— $V(j\omega)$
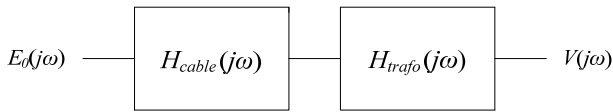
Fig. 7. Block diagram of the cable connected to the transformer winding.

In this figure:

$H_{cable}(j\omega)$ is the cable transfer function shown by (20)
$H_{trafo}(j\omega)$ is the transformer transfer function
$E_0(j\omega)$ is the excitation voltage function
$V(j\omega)$ is the voltage at the transformer

Depending on which computation is performed (STLM) or (MTLM) the output voltage $V(j\omega)$ refers to the voltage at a layer or at a turn of the transformer. The transfer functions of the transformer are already known from previous situation without cable. The total transfer function of the inter-connected cable in series with the transformer is simply the multiplication of both transfer functions. Like the situation without cable, the input excitation voltage is set equal to unity to get the transfer function in frequency domain at the output (impulse response).

VI. COMPUTATION RESULTS WITH CABLE ADDED

For the situation with cable added, there is no comparison of computations with measurements as it was in the case without cable. The only verification are the similarities between the computed and measured characteristic impedance of the cable (about 14 Ohm) and propagation delay. In Figures 8 and 9 the inter-turn voltage distributions for turns 1-20 and turns 80-100 respectively of the first layer are shown. The computed propagation time can be read from the figures and is about 0.6 µs. The peak value of the inter-turn voltage is higher than in the situation without cable.
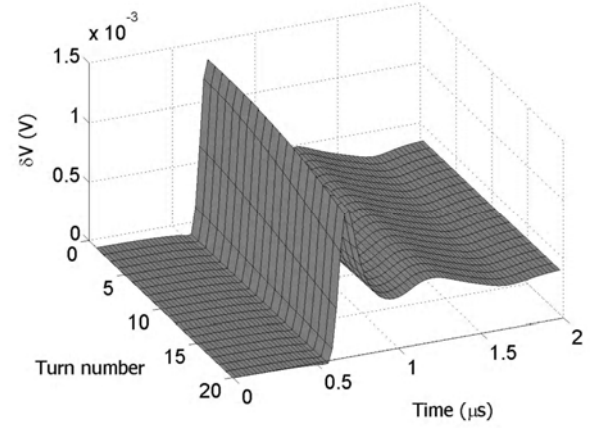

Fig. 8. Computed inter-turn voltage distribution of turn 1-20 in the first layer with inter-connected cable.
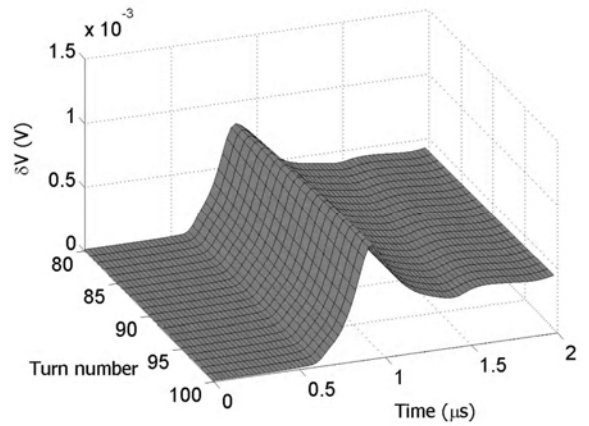

Fig. 9. Computed inter-turn voltage distribution of turn 80-100 in the first layer with inter-connected cable.

VII. CONCLUSIONS

The hybrid model can be used with full success for determination of voltage distribution in layer-type transformer windings. This was verified on an actual transformer. Computed voltage transients show good agreement with measurements. The cable is modeled by extracting its transfer function and taking into account a complex dielectric permittivity. Different results for an input step function are presented with and without applying a cable between the source and the transformer. It is remarkable that the peak inter-turn voltage for the situation with cable is just increased. A reason for this is because there will occur reflection when the traveling wave reaches the transformer terminal, caused by the difference in characteristic impedance of the cable and the transformer winding section. The reflected wave will be added to the incident wave. As a result, the voltage amplitude at the transformer terminal can increase significantly. As a consequence, the inter-turn voltage will also be higher.

VIII. APPENDIX

The elements [5] of the sub matrices in (6) for N_c coils are

Sub-matrix **AU** [$(N_c+1)\times N_c$]:
$AU_{i,i} = -1$, for $i \neq 1$ and $AU_{i,i} = 1$, for $i=1$
$AU_{i,i-1} = \exp(-\Gamma_{i-1}l_{i-1})$, for $i=2,3,\ldots,N_c+1$

$AU_{i,j}=0$, otherwise

Sub-matrix **BU** $[(N_c+1)\times N_c]$:
$BU_{i,i}=-1$, for $i\neq 1$ and $AU_{i,i}=1$, for $i=1$
$BU_{i,i-1}=\exp(\Gamma_{i-1}l_{i-1})$, for $i=2,3,\ldots,N_c+1$
$BU_{i,j}=0$, otherwise

Sub-matrix **AI** $[(N_c-1)\times N_c]$:
$AI_{i,i}=\exp(-\Gamma_i l_i)$, for $i=1,2,\ldots,N_c-1$
$AI_{i,i+1}=-z_i/z_{i+1}$, for $i=1,2,\ldots,N_c-1$
$AI_{i,j}=0$, otherwise

Sub-matrix **BI** $[(N_c-1)\times N_c]$:
$BI_{i,i}=-\exp(\Gamma_i l_i)$, for $i=1,2,\ldots,N_c-1$
$BI_{i,i+1}=z_i/z_{i+1}$, for $i=1,2,\ldots,N_c-1$
$BI_{i,j}=0$, otherwise
$RU_{1,1}=(1-k_1)E_0$, $RU_{i,1}=(k_i-k_{i-1})E_0$, for $i=2,3,4,..,N_c$ and
$RU_{i,1}=-k_iE_0$ for $i=N_c+1$
$RI_{i,1}=0$, for $i=1,2,3,\ldots,N_c+1$

For a particular coil with N turns, the matrix in (6) is of order $2N\times 2N$ and the elements are

Sub-matrix **MA** $[(N+1)\times N]$:
$MA_{i,i}=1$, for $i=1$ and $MA_{i,i}=-1$, for $i=2,3,\ldots,N$
$MA_{i,i-1}=\exp(-\Gamma a)$, for $i=2,3,\ldots,N+1$

Sub-matrix **MB** $[(N+1)\times N]$:
$MB_{i,i}=1$, for $i=1$ and $MB_{i,i}=-1$, for $i=2,3,\ldots,N$
$MB_{i,i-1}=\exp(\Gamma a)$, for $i=2,3,\ldots,N+1$

Sub-matrix **MC** $[(N-1)\times N]$:
$MC_{i,i}=C_{i+1,i}-C_{i,i}\exp(-\Gamma a)$ for $i=1,3,\ldots,N-1$
$MC_{i+1,i}=-C_{i+1,i}\exp(-\Gamma a)$, for $i=1,3,\ldots,N-2$
$MC_{i-1,i}=C_{i,i}-C_{i-1,i}\exp(-\Gamma a)$ for $i=2,3,\ldots,N$
$MC_{i-1,i+1}=C_{i,i+1}$ for $i=2,3,\ldots,N-1$

Sub-matrix **MD** $[(N-1)\times N]$:
$MD_{i,i}=C_{i+1,i}+C_{i,i}\exp(\Gamma a)$ for $i=1,3,\ldots,N-1$
$MD_{i+1,i}=C_{i+1,i}\exp(\Gamma a)$, for $i=1,3,\ldots,N-2$
$MD_{i-1,i}=-C_{i,i}+C_{i-1,i}\exp(\Gamma a)$ for $i=2,3,\ldots,N$
$MD_{i-1,i+1}=-C_{i,i+1}$ for $i=2,3,\ldots,N-1$

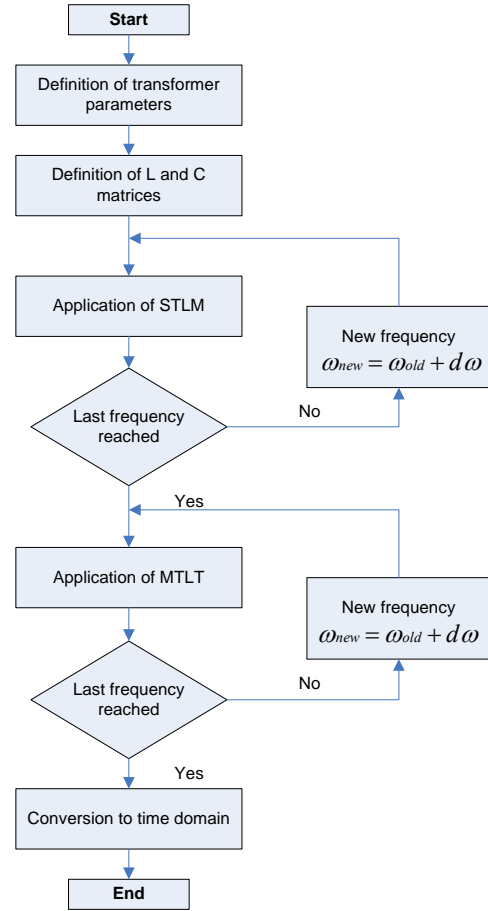In the above expressions, $l_i=N_i a$ is the length of the *i-th* layer.

Fig. 10. An algorithm for inter-turn voltage computation.

IX. References

[1] T. Craenenbroek, J. De Ceuster, J. P. Marly, H. De Herdt, B. Brouwers, and D. Van Dommelen, "Experimental and numerical analysis of fast transient phenomena in distribution transformers," in IEEE Power Eng. Soc. Winter Meeting, Singapore, Jan. 2000.

[2] M. Popov and L. van der Sluis, "Improved calculations for no-load transformer switching surges," *IEEE Trans. Power Delivery*, vol. 16, pp. 401–408, July 2001.

[3] G. Paap, A. Alkema, and L. van der Sluis, "Overvoltages in power transformers caused by no-load switching," *IEEE Trans. Power Delivery*, vol. 10, pp. 301–307, Jan. 1995.

[4] K. Cornick, B. Filliat, C. Kieny, and W. Müller, "Distribution of very fast transient overvoltages in transformer winding," in *CIGRE*, Paris, France, 1992, paper 12-204.

[5] M. Popov, L. van der Sluis, G. C. Paap and H. de Herdt: "*Computation of Very Fast Transient Overvoltages in Transformer Windings*", IEEE Transactions on Power Delivery, Vol. 18, No.4, October 2003, pp.1268-1274.

[6] Y. Shibuja, S. Fujita, N. Hosokawa: "Analysis of Very Fast Transient Overvoltages in Transformer Winding", *IEE Proceedings on Generation Transmission and Distribution*, Vol.144, No. 5, September 1997, pp.461-468.

[7] J.P. Bickford J.P., N. Mullineux, J.R. Reed: "*Computation of Power System Transients*", IEE, Peter Peregrinus Ltd., 1976, ISBN 0901223859.

[8] G. Mugala, R. Eriksson: "High frequency characteristics of a shielded medium voltage XLPE cable", Annual Report Conference on Electrical Insulation and Dielectric Phenomena, 2001, pp. 132-136.